International Journal of Heat and Technology
Vol. 44, No. 2, April, 2026, pp. 690-702
Journal homepage: http://iieta.org/journals/ijht

Bridge Pier Scour Mechanisms Under Complex Flow Conditions: A Numerical Case Study of the Tikrit Bridge

Dalia Sh. Mahdi[1], Mohammed Khairullah Ahmed Al-Dorry[2], Asmaa Abdul Jabbar Jamel[1*], Muataz I. Ali[3]

[1] Department of Dams and Water Resources Engineering, Tikrit University, Salah al-Din 34001, Iraq
[2] Department of Civil Engineering, Tikrit University, Salah al-Din 34001, Iraq
[3] Department of Civil Engineering, University of Samarra, Salah al-Din 34001, Iraq

Corresponding Author Email: ms.asmaajameel@tu.edu.iq

https://doi.org/10.18280/ijht.440222

Received: 5 December 2025
Revised: 15 March 2026
Accepted: 28 March 2026
Available online: 30 April 2026

Keywords:
scour, bed-load, critical velocity, grid convergence index, shear velocity

ABSTRACT

Scour around bridge piers is a significant engineering challenge and has become an international phenomenon that causes instability in hydraulic structures, not only for uniform flow but also for complex flow. The purpose of this study is to enhance the understanding of the impacts of turbulent flow and sediment transport on bridge stability by modeling the scour around the piers of Tikrit Bridge in Salah al-Din Governorate. This research aimed to investigate the effects of sediment bed-load flow and clean water flow, and to assess the impact of piers and the spacing between piers on flow patterns and scour dynamics. The findings show that scour intensity is mainly controlled by pier position within the flow field. The upstream front-row piers, which directly face the incoming high-velocity flow, recorded about 48% greater scour under clean-water conditions compared with the front row of the downstream group located in a lower-velocity zone. Under live-bed conditions, this spatial contrast became much stronger, with scour increasing from nearly 0.12 m in the downstream group to about 0.26 m in the upstream front row) 112.5% increase), highlighting the importance of turbulent flow in sediment mobilization and the corresponding impact of scour in high-velocity regions.

1. INTRODUCTION

Transport and Mobility Infrastructure consists of bridges, which are an integral part of the primary infrastructure required for the various modes of transport and mobility. Surprisingly, on many occasions, the stability and longevity of bridges are prejudiced by environmental aspects, specifically hydraulic effects related to the scour at the bridge foundation. Scour refers to the erosion of soil, sand, or gravel around bridge supports due to rapid water movements. Scour at the bridge foundation is a significant concern, mainly during times of flooding or heavy current. Scour causes weakening of the foundation supporting the bridge and poses a threat to its overall stability. Scour depth depends on several factors, including the velocity of the water, the shape of the foundation, the type of soil, and the location of the foundation, among others. Studies have determined that rounded or cylindrical piers are less prone to scour compared to square piers, and structures founded at river bends are more susceptible to the scour process [1]. There is a need for advanced mathematical and hydraulic modeling to be carried out in determining scour predictions under changing flow conditions. This can be done mainly through the use of computational software, such as FLOW-3D, which can accurately predict scour. Shear stresses usually cause scour due to high-velocity flows near the foundations, which leads to bed erosion on the river floor, resulting in the foundations becoming exposed or having less soil cover, ultimately causing the bridge to become unstable [2]. A downward flow that is heavy on the pier front will cause a growing vortex to form, which in turn can lead to erosion that reveals foundations, potentially resulting in the collapse of the bridge and causing injuries [3]. A composite pier consists of piles, a pile cap, and one or more columns, which can be either vertical or sloping [4]. Furthermore, the scour around complex foundation structures, such as composite piers, is further complicated by interactions between the flow structure, including vortices and bottom currents [5].

Research shows that the Superposition Method is effective in estimating the total scour depth for composite piers [6]. In comparative experiments, it was evident that a single pier causes less scour than multiple arrangements, whereas an elliptical shape decreases the intensity of scouring [7]. Other investigations have focused on the effect of sediment size and pier geometry. It has been found that large estimating sediment roughness causes a decrease in scour depth. In another study, the use of an empirical relation yields better prediction [8]. Further experimental investigation has been conducted to examine the pier cover conditions, including cover height and thickness, in order to control scour [9]. It has been shown that the scour depth in river bends tends to increase as the pier angle increases, although blunt-nosed piers are more effective

than square-nosed ones [10]. It is also found that debris significantly affects scour; it enhances scour under shoaling flows, while debris reduces scour under deep flows [11]. Numerical simulations based on these physical experiments show that scour patterns are strongly influenced by the pier shape and the channel width in which the bridge is sitting [12].

Regarding the scour of composite piers, tests confirm the significant role of the pile cap elevation. Maximum scour occurs when the pile cap is partially embedded in the deposits. In contrast, minimum scour is generated when the cap is raised [13]. The current predictions of scour under piers by various scour analyses have a limited range of pier and flow conditions. Detailed guidelines have been proposed to improve them [14]. Although many studies have examined scour around conventional single piers, minimal research has focused on multi-pier bridge configurations in which several piers interact simultaneously with the incoming flow. Such configurations create compound turbulence, intensified horseshoe vortices, and flow contraction effects that cannot be captured using single-pier assumptions. This gap is especially relevant for real bridges such as the Tikrit Bridge, where the piers are arranged in closely spaced groups that significantly alter the hydraulic and sediment-transport conditions. Thus, there is a strong need for further studies to investigate the scouring behaviour under such complex structures, particularly under various hydraulic conditions. This research aims to bridge the gap by investigating scour around pier complexes of a compound bridge, using the northern Tikrit Bridge as a case study. The objective of this study is to investigate scour development around the closely spaced pier groups of the Tikrit Bridge under both clean-water and live-bed flow conditions. The study examines how flow velocity, turbulent structures, and pier spacing influence scour intensity, and employs the equivalent-pier method to calibrate and improve the reliability of the numerical model.

2. STUDY AREA (NORTHERN TIKRIT BRIDGE)

The research was carried out on the Northern Tikrit Bridge, in the northeast part of Tikrit City, and is the bridge linking the centre of the governorate to the Al-Alem district on the east side. The bridge is located at coordinates (Latitude = 34.6798°), (Longitude = 43.6641°), and (Altitude = 91.3368 meters above sea level). The total bridge length is 845 m, while its width is 22.5 m, with two lanes in both directions. For the numerical analysis, a transverse section containing two consecutive pier groups—ten piers in total (A1–A5 and B1–B5)—was selected from the central portion of the bridge. The first group forms the upstream group facing the incoming flow, while the second group lies immediately downstream. This section coincides with the highest-velocity zone of the river cross-section, where flow contraction, wake interaction, and vortex formation are most intense, making it the hydraulically critical region governing scour development at the bridge. The bridge specifications are presented in Figure 1.

(a)

(b)

Figure 1. Study area (Northern Tikrit Bridge)

3. BASIC EQUATIONS FOR LOCAL SCOUR

The Flow-3D is utilized in resolving the complex three-dimensional equations of water flow around bridge piers, as well as sediment transport processes. The software analyzes sediment transport through the simulation of processes of erosion, processes of sedimentation through the evaluation of the effects of velocity, pressure, and changes in water circumstances through the solution of three-dimensional equations, coupled with water flow and transport simulations of sediment, in order to determine water current effects on sediment and the composition of soils. The software is built on numerical analysis, involving the use of advanced methodologies to increase the accuracy of the results generated. Flow-3D offers effective instruments in the understanding of water and sediment interactions around structural features, such as bridges. This is achieved through:

- Calculating suspended sediment transport.
- Calculating sediment deposition due to gravity.
- Calculating sediment entrainment due to shear layers and flow turbulence.

Calculating bed-load transport, where sediments roll, within this framework, FLOW-3D computes the suspension (lift) velocity using the formulation of Mastbergen & Van den Berg [15] (Eq. (1)), while the particle settling velocity and Shields-related parameters follow the experimentally validated relations of Soulsby [16] (Eqs. (2)-(5)).

$$u_{lift},i \;=\; \alpha\,\eta\; d_*^{0.3}(\theta_i - \theta_{cr},i)^{1.5}\sqrt{g\,\frac{d_i(\rho_s,i-\rho_f)}{\rho_f}} \qquad (1)$$

$$u_{settling},i \;=\; \frac{V_f}{d_i[\,(10.36^2+1.049\,d_*,i^3)^{0.5}-10.36\,]} \qquad (2)$$

And Dimensionless Particle Diameter by Eq. (3):

$$d_*,i \;=\; d_i\left[\frac{(\rho_f(\rho_s,i-\rho_f))}{\mu_f^2}\right]^{\frac{1}{3}} \qquad (3)$$

While shear stress and critical shear stress are defined by Eqs. (4) and (5), respectively [17, 18].

$$\theta_i = \frac{\tau}{|g|d_i(\rho_s,i-\rho_f)} \qquad (4)$$

$$\theta_{cr},i \;=\; \frac{0.3}{1+1.2\,d_*,i} + \;0.055\,[\,1\;-\exp(-0.02\,d_*,i)] \qquad (5)$$

The Shields coefficient and the critical Shields coefficient θ_r, θ_{cr}. It is calculated from Eqs. (4) and (5) by Soulsby and Whitehouse, respectively. These formulations were selected because they are standard models for sand-bed rivers, fully compatible with FLOW-3D's sediment transport algorithms, and explicitly incorporate turbulence-driven entrainment and non-linear settling behaviour. These characteristics align with the hydraulic regime and sediment properties at the Tikrit Bridge, making them suitable for predicting local scour development.

4. NUMERICAL MODELLING IN THREE-DIMENSIONAL FLOW

The dimensions of the bridge pier model for this study were designed to match a scaled-down version of the original bridge model. The model was divided into three computational domains extending from top to bottom (as shown in Figure 2). Whether the model is used for water flow (clean water) or sediment scour modelling (bed-load), the Size of the computational domain primarily depends on the diameter of the pier (D).

In this study, the lateral width of the computational domain was set to 10.5 D, with the longitudinal axis of the pier centred in the middle of the domain, allowing for the neglect of the effect of the tank wall contraction on the central region of the domain. The total length of the model for the study area was set to 22 D, with the axial centre of the front pier located 11 D from the inlet boundary and the axial centre of the rear pier located 11 D from the outlet boundary. This arrangement ensures that the water flow in the region, both before and after the pier, remains unaffected, allowing for the full development of the flow without disruption or interference [18].

To ensure the stability of the water flow and prevent soil erosion, fixed solid barriers with the same width and height (as defined by the red area) were placed in the upstream and downstream regions of the bed for the bed-load model.

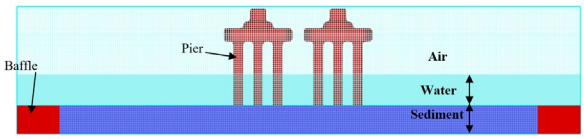

(a) Section I

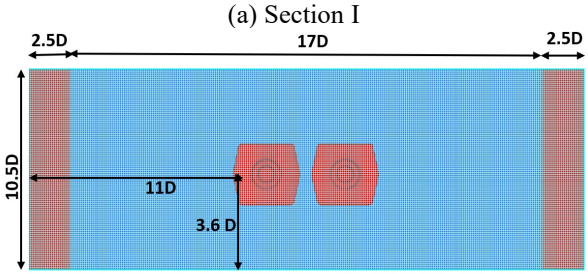

(b) Section II

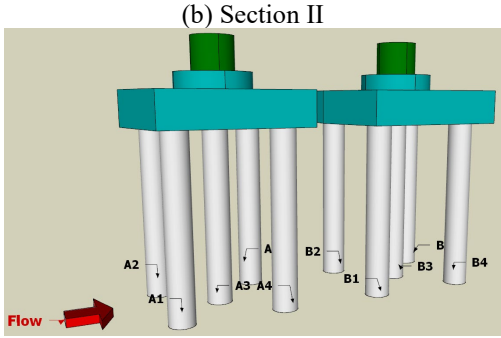

(c) Current study

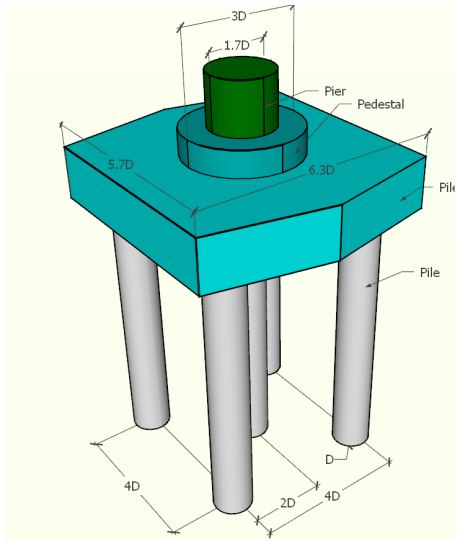

(d) Current study

Figure 2. The numerical model

5. FLOW CONDITIONS (BED-LOAD AND CLEAR WATER)

The scour due to flow is divided into two main types, depending on the flow conditions and sediment movement over the structure. The clean-water scour refers to the scour occurring under the conditions of no sediment motion on the horizontal layer above the structure. Here, sediments remain stationary or immobile while the water flow continues to impact the surface.

On the other hand, if the sediments over the structure are in motion, the scour is termed as live-bed scour. Scour of this nature occurs where the water velocities are such that sediment transport is achieved; hence, much greater effects on the structure's surface will take place. Scour is usually classified according to whether the velocity of flow is less or greater than the critical velocity for sediment transport. This critical velocity refers to the requisite velocity at which sediment on the structure's surface may initiate motion. Suppose the flow velocity is less than the critical sediment velocity. In that case, the scour is referred to as clean-water scour, where the sediments remain stationary, but the water has a greater impact on the surface.

Suppose the flow velocity is less than the critical sediment velocity. The scour, in that case, will be termed clean-water scour, where the sediments are at rest, while the water can have more pronounced effects on the surface.

If the flow velocity is greater than the critical sediment velocity, the scour is referred to as live-bed scour, where sediments move and contribute to scour on the surface of the structure.

Based on the characteristics of sediment development in the riverbed, a coupled water-sediment model was developed. The engineering specifications and hydraulic parameters are detailed in Table 1. The V/Vc values were computed using the actual sediment properties of the Tigris River bed reported by Yass and Al-Tikrite [19], where the surface and subsurface layers have D50 ≈ 34 mm and 14 mm, respectively. The critical velocity Vc was obtained using the Shields-based relations and Soulsby formulation adopted by Flayyih et al. [20], ensuring consistency with the FLOW-3D sediment transport model.

Table 1. The engineering specifications and hydraulic variables of the model

Numerical Model	Scouring Environment	Pier Diameter (cm)	Water Depth (cm)	V/Vc	Fr
A	Clean water	15	25	0.80	0.15
B	Live- bed	15	25	1.20	0.23

6. PIER SCOUR ANALYSIS PROCESS

To simulate the scour depth around the bridge piers and obtain accurate results, several steps were implemented. Figure 3 is a flowchart that illustrates the basic procedural steps for simulating three-dimensional flow.

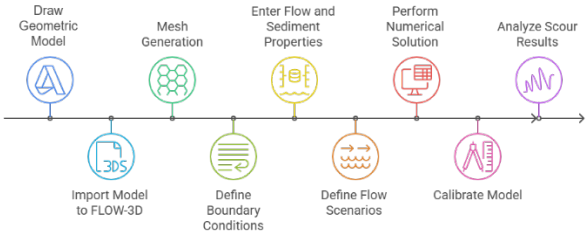

Figure 3. Pier scour analysis process

7. NUMERICAL METHODOLOGY

Flow-3D offers several advanced physics options; however, only four physics activations are considered necessary to achieve an accurate simulation for the data required in this study. The gravity option is activated with gravitational acceleration in the vertical direction, along with activating the sediment erosion model using the critical shields number and the bed-load transport coefficient. Other sediment parameters remain at their default values. Additionally, the viscosity and turbulence options are activated, with Newtonian viscosity applied to the flow, alongside the selection of the appropriate turbulence model. After fully setting up the model, the Renormalization Group (RNG) turbulence model is applied in this study, as it is chosen as the turbulence model for simulating turbulent flow.

Appropriate boundary conditions that correspond to the physical conditions of the model were applied. The inlet boundary condition was set with a discharge flow rate (Q) at the beginning of the channel. At the model's outlet, external water pressure (Pressure) was applied as a function of water head (Water Head) to prevent the outlet boundary effects from influencing the simulation results in the final step [21]. For the no-slip conditions used at the bed boundaries, the tangential and normal velocities are set to zero (u = v = w = 0), where u, v, and w represent velocities in the x, y, and z directions, respectively. By applying the no-slip conditions, the wall conditions are defined so that the average velocity of turbulent flow at a given point corresponds to the natural logarithm of the distance from that point to the fluid region boundary.

Additionally, logarithmic velocity boundary conditions are employed to calculate the shear stress on all no-slip wall boundaries, in conjunction with the turbulence model used in the simulation. The standard atmospheric pressure (Pressure) was applied at the top of the simulation region. Figure 4 illustrates the model used in the current study, along with its associated boundary conditions.

The most important factor to consider in modelling Flow-3D is determining the computational mesh, which primarily depends on the Size of the domain defined and the number of cells, both of which affect runtime and solution accuracy. Unknown values are calculated by dividing the actual working space into smaller, interconnected cells, and then computing the value at the centre of each cell. The optimal number of cells can be obtained by representing obstacles using the percentage of area/volume. The FAVOR option is a compelling method for incorporating the effects of geometry into the governing equations. Since the cells are orthogonal, the optimal cell size must be determined to generate a system that closely resembles the actual situation. If the cell sizes are not ideal, problems may occur in geometric modelling, as illustrated in Figure 5. To avoid these issues, the FAVOR option enables users to obtain precise geometric shapes, allowing for mesh-independent results. Three different mesh sizes were used, and the Grid Convergence Index (GCI) methodology was employed to determine the optimal mesh size. This method is recommended for evaluating the estimation error. Three different computational grids were applied to choose the appropriate mesh.

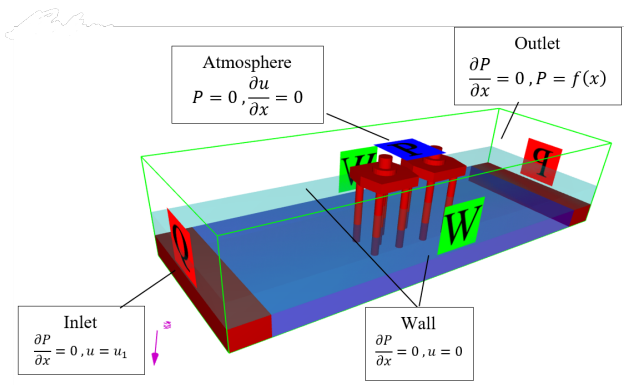

Figure 4. Boundary conditions (Current study)

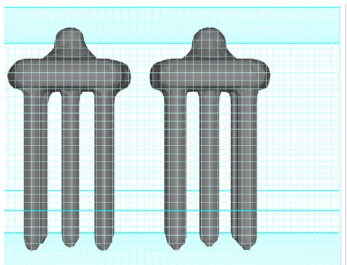

(a) Size cells 0.03 mm

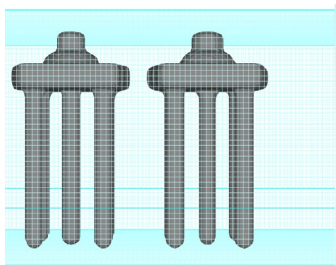

(b) Size cells 0.02 mm

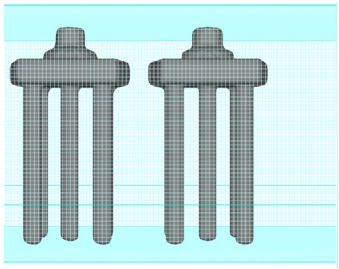

(c) Size cells 0.015 mm

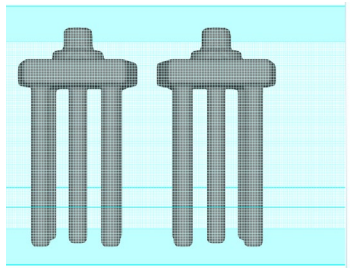

(d) Size cells 0.01 mm

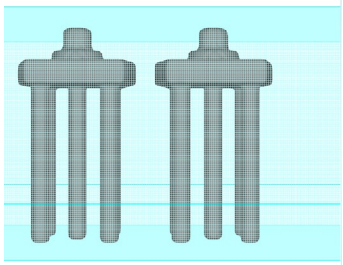

(e) Size cells 0.008 mm

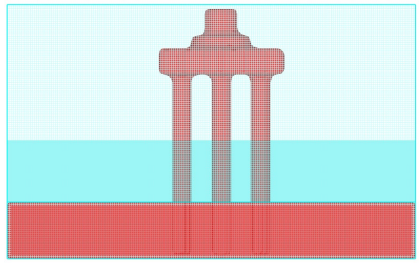

(f) Final model with 0.01 mm

Figure 5. FAVOR option with different cell sizes

Table 2. Mesh properties test in grid convergence analysis, calculating grid convergence index

Type	Block Size (cm)	Mesh	p	GCI12	GCI23	Asymptotic Range
1	0.017	Coarse				
2	0.013	Medium	5.99	0.002	0.010	1.014
3	0.01	Fine				

The flow depth rate for the sloped channel was also used at six different locations in the FLOW-3D program to assess the accuracy of the mesh. The convergence accuracy p can be calculated as shown in Eq. (6):

$$p = \ln\left(\frac{f_3 - f_2}{f_2 - f_1}\right) \Big/ \ln(r) \tag{6}$$

where, f_1, f_2, and f_3 are the indicators obtained from the FLOW-3D simulation corresponding to the coarse mesh, and r is the accuracy ratio. The fine GCI is defined as in Eq. (7) [22]:

$$GCI_{fine} = \frac{1.25\,|\varepsilon|}{r^p - 1} \tag{7}$$

where, $\varepsilon = \frac{f_2 - f_1}{f_1}$, is the relative error, and f_2 and f_3 are the solutions for the medium and fine meshes, respectively. Thus, dimensionless indicators GCI12 and GCI23 can be calculated as in Eq. (8):

$$GCI_{12} = \frac{1.25\left|\frac{f_2 - f_1}{f_1}\right|}{r^p - 1} \tag{8}$$

Mesh independence is verified by calculating the GCI using Eqs. (6)–(8), as shown in Table 2. Since the GCI values for the fine mesh (GCI12) are small compared to the coarse mesh (GCI23), it can be concluded that the mesh has been obtained optimally, and no further adjustments to the mesh are necessary.

The calculated values for $\mathrm{GCI}_{23}/\mathrm{r}^p\mathrm{GCI}_{12}$ are close to 1, indicating that the numerical solutions fall within the asymptotic range. As a result, the mesh consists of cells with a size of 0.01 cm, see Table 2.

8. VERIFICATION USING THE EQUIVALENT PIER METHOD

The methodology is based on several assumptions. First, the structure can be divided into a maximum of three components. Then, for scour calculation, each component can be replaced with a single circular pier penetrating the surface with an effective diameter (D) that depends on the shape, Size, location, and orientation of the component relative to the flow. For the components initially buried, the effective diameter will also depend on the amount of sediment removed by the components located above the bed. Finally, the effective diameters of the structural components are added together to obtain the effective diameter of the entire structure (i.e., the presence of one component does not affect the effective diameter of the other components), as shown in Figure 6. If the primary interactions are identified and considered, acceptable estimates of the equilibrium scour depth can be achieved. The equations are designed to be applicable in any logical combination of components (for example, combining a pier with a set of piers without the pier cap is not allowed) and for all practical ranges of their locations. Since the equations are empirical and cover a wide range of conditions, they may not provide consistent results when pushed to their limits, such as evaluating a pier as a group of piers penetrating the water surface, rather than a single pier.

To calculate the scour depth around bridge piers, the following equations are used, taking into account the scour and flow conditions. The critical depth is calculated using Eq. (9), where the safety factor (SF) is typically set at 1.25 to provide conservative estimates of scour depth.

$$D*_{\{cs\}} = SF \times \left(D*_{\{col\}} + D*_{\{pc\}} + D*_{\{pg\}}\right) \tag{9}$$

Clean-Water Scour, when there is no sediment transport, is

calculated by Eq. (10):

$$d_s = D*_{\{cs\}} \times \left(2.0 + 0.4 \ln\left(\frac{D}{D*_{\{cs\}}}\right)\right) \quad (10)$$

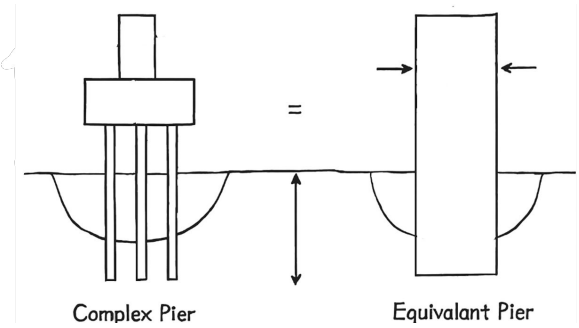

Figure 6. Equivalent pier

Live-bed scour occurs when sediment transport is present, and is calculated using Eq. (11):

$$d_s = D^*_{\{cs\}} \times \left(1.3 + 0.6 \ln\left(\frac{D}{D^*_{CS}}\right)\right) \times \left(\frac{U}{U_t}\right)^{\{0.2\}} \quad (11)$$

$\frac{U}{U_t}$ is the Flow Intensity Factor, defined as the ratio of the approaching flow velocity U to the critical velocity U_t needed to transport sediment [22, 23].

9. VERIFICATION OF SCOUR RESULTS

Figure 7 and the associated radar plots provide a quantitative verification of the numerical model by comparing the FLOW-3D scour predictions with established formulations, including Khwairakpam et al. [24], Sheppard et al. [25], Khafsa and Ahmed [26], FHWA-HIF [22], in addition to the FDOT equivalent-pier methods (Eqs. (9)–(11)). For clear-water conditions, the numerical model achieved the lowest errors among all methods (MAE = 0.25, RMSE = 0.31, MAPE = 14.8%, SI = 0.42), whereas the closest empirical formulation was Sheppard (2004) (MAE = 0.35, RMSE = 0.41). Under live-bed conditions, the FLOW-3D results similarly produced the most accurate performance (MAE = 0.67, RMSE = 0.74, MAPE = 18.2%, SI = 0.51), with the nearest agreement appearing in the study of Khafsa and Ahmed [26]. According to the results presented, this numerical model has been demonstrated to exceed existing calculations consistently. The numerical model is a reliable and viable tool for simulating complex multi-pier configurations for scouring prediction based on strong correlations with the established FDOT equivalent pier technique. Numerical model data consistently exceeds that of existing equations regardless of whether or not pier group interaction and spacing was considered.

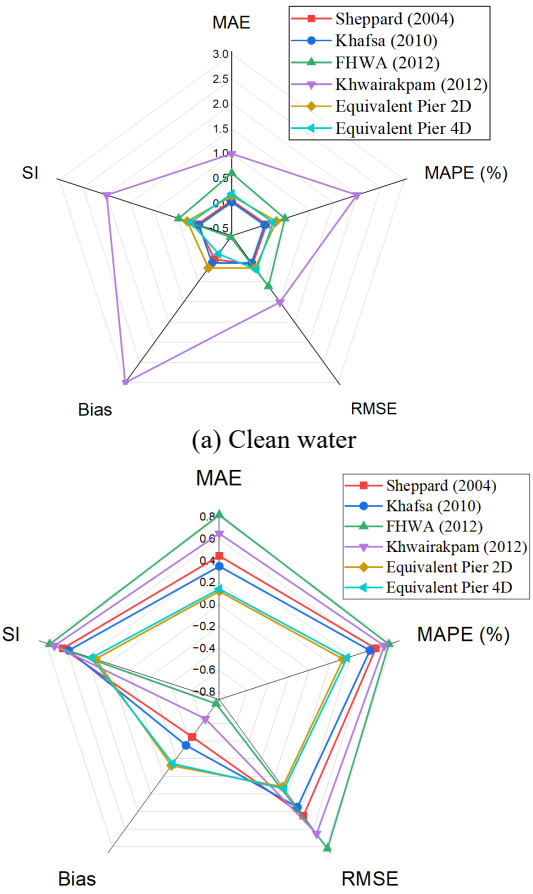

Figure 7. Calibration of the current study model with previous studies

10. SCOUR AROUND THE PIERS

10.1 Effect of multiple piers on scour (Top view)

According to the FLOW-3D simulation results, the impact of scour around a set of supports was examined under both clean-water and bed-load conditions, with a specific focus on the impact of support distribution on the turbulent flow regime and scour. The results, as shown in Figure 8, show deeper scour at the upstream front-row piers under bed-load flow, demonstrating that the presence of multiple supports significantly enhances turbulence in the flow regime and increases the scouring influence compared to a single support. This is due to the complex interaction between the flow and the numerous peripheral surfaces of the supports.

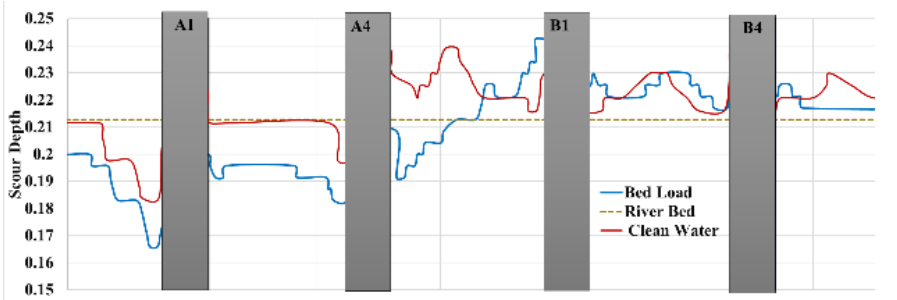

Figure 8. The change in the riverbed for the right-side section of the study area

In the clean-water condition, the upstream front-row piers located in the high-velocity zone experienced an average scour depth of about 0.37 m, compared with approximately 0.25 m around the downstream piers located in a lower-velocity zone. This represents an increase of roughly 48% and reflects the effect of exceeding the local critical velocity for sediment motion. This sudden change in scour is due to the fact that the flow velocity in these regions is greater than the critical velocity for sediment mobilization, which increases the sediment-carrying capacity of the water and results in higher erosion near the support surfaces. The influence of the turbulent flow creates eddies around the supports that further mobilize the sediments and increase the scour. Under bed-load conditions, the contrast became more pronounced. Scour depth increased from about 0.12 m around the downstream piers to approximately 0.26 m around the upstream front row, corresponding to a 112.5% increase. This deeper scour results from the combined influence of turbulence and active sediment mobility, which enhances sediment entrainment near the upstream piers. The severe variation in the scour is a result of the effect of turbulent flow that generates eddies within the regions surrounding supports. They increase the interaction between flow and sediments, enhancing the water-carrying capacity and leaving sediments on the surface, thereby intensifying the effect of scour.

The presence of multiple supports complicates flow dynamics, as the interaction between turbulent flow and eddies generated by each support reduces flow stability and increases sediment transport. The interaction is more prone to scour in the regions surrounding multiple supports as the eddies increase pressure around the surfaces, facilitating increased mobilization of sediment. On the other hand, a single support will tend to concentrate the flow at a single point, limiting the scour effect compared to the experience of many supports.

10.2 Effect of multiple piers and flow type on scour and deposition (Side view)

One central point made was that the scour and deposition around bridge supports, both bed-load and clean-water, were studied. What was gained from this is that the very different scour and deposition behavior of bed-load and clean-water can be observed, arguing for the dynamic interaction of flow velocity and turbulent flow around the piers. As shown in Figure 8, in case of cleawater scenario, the scour within the neighborhood of the piers A1 and A4, which concern the high velocity region, is higher, as compared with the other points, due to the flow velocity over here exceed the critical velocity that can cause the particles to begin to move, hence the turbulent flow raises the particles above the adjacent surfaces of the supports and there is loss of particles at these places. However, as the distance from the piers increases, the flow velocities decrease (in a low-velocity region), resulting in a decrease in scour because these regions cannot transport particles effectively. On the other hand, under bed-load conditions, where the turbulent flow and the sediments meet each other on the bed, the scour will be significantly higher, as compared to the clean water condition, at the points A1 and A4 of the piers, because in these cases the particle transportation by the turbulent flow is very high, as compared with the rest of the forces, which enhances the flow to transport or move the particles above the adjacent surfaces of the supports, thus resulting higher scouring at these points. However, as the distance from the piers increases, the bed becomes narrower and narrower. Hence, the force of the flow decreases, and the flow begins to lose the power to carry the particles. Thus, the particles begin to deposit at locations with low flow velocity. The reason for deposition in these areas is the reduced flow velocity, which is not strong enough to transport the sediments; hence, the sediment settles where the velocity is lower than the critical velocity. Scour, and this phenomenon works in a complex manner: while high flow scours sediments from a particular area, low flow scours sediments from other areas, resulting in deposition. These observations suggest that scouring is mainly done in areas of high flow velocities where the flow has enough capacity to mobilize and transport sediments from around supports. Deposition occurs in areas of low flow velocities where the flow cannot mobilize sediments and thus deposits them in these still regions. This interaction between scour and deposition aptly describes the dynamic effects of flow on the stability of bridges in sediment-laden environments. The study, among other things, recommends that the effects of deposition and scour should be taken into consideration in the design of multi-supported bridges, especially those in sediment-carrying flow conditions, for structural stability and prevention of unfavourable performance over the long term.

10.3 Effect of multiple supports and flow type on scour and deposition (Front view of flow)

The effects of deposition and scour surrounding bridge piers were examined under conditions of bed-load and clean water. Figure 9 Shows limited scour around the mid-channel piers, indicating that they lie in a low-velocity, low-turbulence region, exemplified by A1 and A4, and the inner piers, represented by A3 and B3, which can be attributed to the differing flow velocities and their interactions with turbulent flow. In the outer piers, a deeper scour is faced due to the higher flow velocities concentrated on the lateral sides of the bridge structure. The higher velocities increase the ability of the flow to transport sediments and therefore develop a deeper scour around the supports. The inner piers, however, like A3 and B3, are exposed to smaller flow velocities owing to the equality in flow distribution along the bridge width. Consequently, the scouring effect on the piers diminishes to 10–12% relative to the one faced on the outer piers. This decrease can be attributed to the less active eddies developed from a flow of a turbulent nature within the inner areas, consequently decreasing the ability of the flow to transport sediments.

Under bed-load conditions, where flow interacts with transported sediments, the presence of turbulent flow increases the scour in piers A1 and A4. The higher flow velocities in these regions increase the carrying capacity of the flow, which results in a 15–20% increase in scour compared to the clean water condition. In piers A3 and B3, there is a rise in scour under bed-load conditions; however, it remains negligible due to the lower flow velocities compared to the outer piers. As one moves further from the central piers, flow velocities are not high enough to transport sediments, and deposition starts; the sediments will be deposited in areas with low flow velocity. The findings confirm that scour occurs in cases of high-velocity flow, such as piers A1 and A4, where flow can carry sediments. Low flow velocity in middle piers, like A3 and B3, causes deposition because it is not able to transport sediments continuously. This interaction between deposition and scour shows the necessity of considering the distribution

of flow velocity during the design of bridges in regions that are exposed to regimes of turbulent flow.

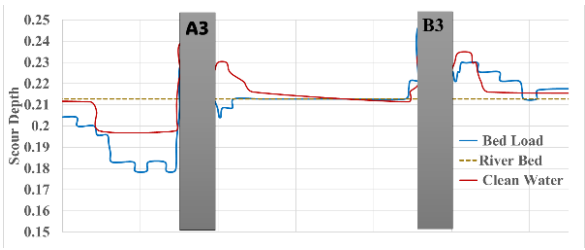

Figure 9. The change in the riverbed for the cross-section of the study area

10.4 Variations in behavior between piers on both sides of the study area (Right and left)

When comparing the piers on the right side, such as A1, A4, B1, and B4 (shown in Figure 10), with the piers on the left side, such as A2, A5, B2, and B5 (shown in Figure 10), there is a notable similarity in the scour and deposition behavior between the two sides. In the clean water condition, scour is more pronounced in the areas near the supports due to high flow velocities, and the effect of turbulent flow is observed similarly on both sides. In the bed-load condition, the flow velocities increase in the areas close to the piers, leading to an increase in scour on both sides by 15–20%. In regions with lower flow velocities, deposition occurs in areas farther from the piers on both sides in a similar manner, where the flow velocity is insufficient to mobilize the sediments. These results indicate that the effects of scour and deposition are symmetrically distributed across the bridge, from left to right.

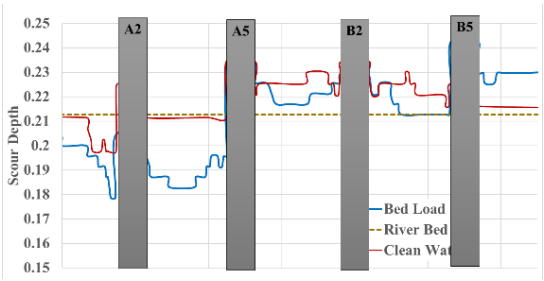

Figure 10. The change in the riverbed of the left bank section of the study area

10.5 Effect of multiple piers on scour (Front view)

Scour behaviour was compared between the front sections of the flow (Figures 11-16), which collectively illustrate the variation of scour depth along the front, middle, and rear piers. The front-row piers consistently show the deepest and most concentrated scour due to their direct and parallel sections (right, left, and central) of the flow (Figures 11-16) for piers A1, A2, B1, and B2. In the front sections, where the piers are exposed to turbulent flow, higher flow velocities are generated due to the formation of strong eddies behind the piers. These elevated velocities significantly enhance the flow's capacity to transport sediments. Under clean water conditions, scour in the front sections is observed to be 15–18% higher than in the parallel sections, attributed to the higher flow velocities that facilitate more effective sediment transport. Under bed-load conditions, where the flow is carrying sediments, scour increases by 18–22% in the front sections compared to the condition with clean water. This is due to the turbulent flow's higher velocities, which further enhance the flow's ability to mobilize and transport sediments, resulting in greater scour.

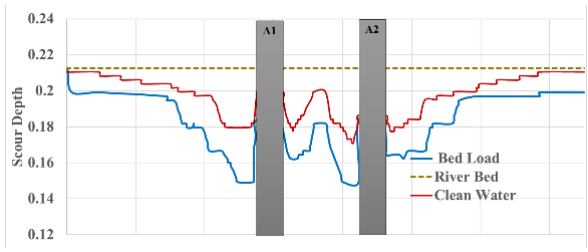

Figure 11. Section A1–A2

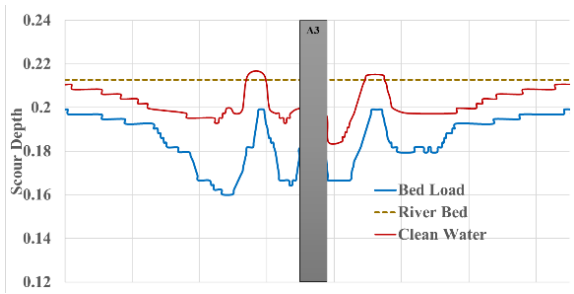

Figure 12. Section A3

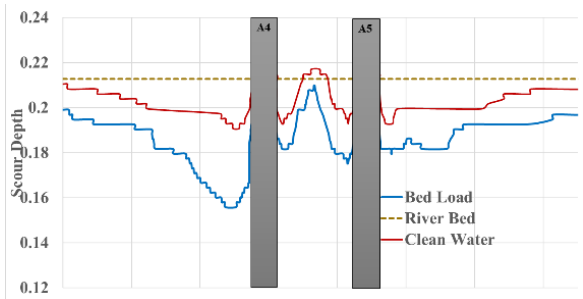

Figure 13. Section A4–A5

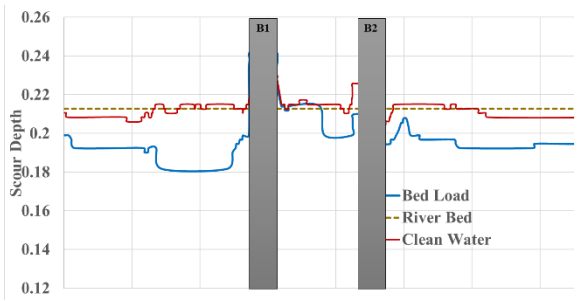

Figure 14. Section B1–B2

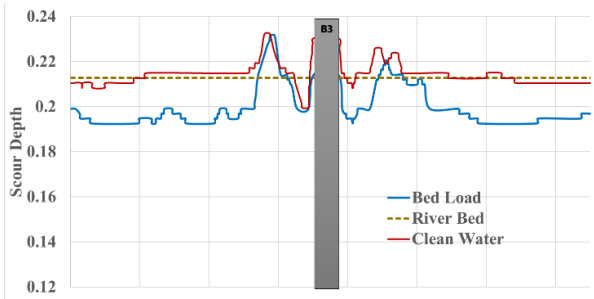

Figure 15. Section B3

In contrast, these regions, in A2 and B2, have fewer scour sites since velocities are lower and flows are generally more evenly distributed across the bridge width. The rise in scour in these regions is approximately 10–14% compared to clean water conditions. The scour is lower here because the velocities of flow in parallel sections are typically below the critical velocity to mobilize the sediments, unlike the front sections. It shows that the prominent scour in the front sections is due to more vigorous turbulent flow. In contrast, the lower velocities in parallel sections contribute to less scour, regardless of whether the conditions are clean water or bed - load.

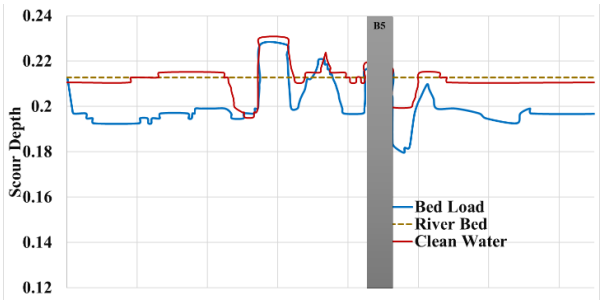

Figure 16. Section B4–B5

10.6 Shear stress distribution around piers

Shear velocity is a fundamental parameter in fluid dynamics, indicating the frictional force between the water flowing in a channel and the surfaces in contact with it. It is one of the most important parameters used to determine a flow's ability to convey sediments and cause local scour near hydraulic structures, such as bridge piers and abutments. Knowledge of the distribution of shear velocity in a river or a channel can be used to predict the impact of turbulent flow on the near-bed stability of subsurface structures, as well as the environmental impact of these structures. Figure 17 shows the cross-sectional shear velocity profiles of the river mid-piers under clean water and bed-load conditions. Under clean-water conditions, shear velocity increases around the pier surfaces due to vortex formation, reaching values of approximately 0.75–0.90 m/s. These elevated values result from the interaction between the incoming flow and the pier group. In regions farther from the piers, shear velocity decreases to nearly 0.2 m/s, reducing the transport capacity of the flow and limiting scour.

Sediment transport under bed-load conditions is associated with greater near-bed shear velocities than under clear-water conditions, resulting in an increase in the maximum shear velocity (1.0 to 1.12 m/s) and therefore an increase in sediment transport capacity and an increase in local scour at pier groups. In contrast, shear velocities are approximately 0.1 m/s at larger distances from the piers, which accounts for less scour in regions of low shear velocity. The difference in shear velocity at the piers between conditions demonstrates that bed-load conditions exhibit greater shear velocities near piers due to increased turbulence and sediment–flow interaction, resulting in higher near-bed shear and greater scour. The lower shear velocity observed in low-velocity locations located far from the piers will decrease sediment transport and therefore decrease scour in both cases.

As it can be seen in Figure 18, the shear velocity is at its highest near piers under clear water conditions due to turbulent flow caused by eddies generated behind the piers, with a maximum shear velocity of 0.288 m/s; whereas, in areas farther from the piers, shear velocity is significantly lower (0.05 m/s), which means the flow within those areas is much more stable and less turbulent. Under bed-load conditions, where the flow carries sediments along, shear velocity near the piers is higher compared to clear water conditions and reaches 0.334 m/s. This constitutes a 16% increase compared to the use of clear water. In areas farther from the piers, shear velocity in the bed-load condition was 0.1 m/s, reflecting a 100% increase compared to the 0.05 m/s observed under clear water conditions.

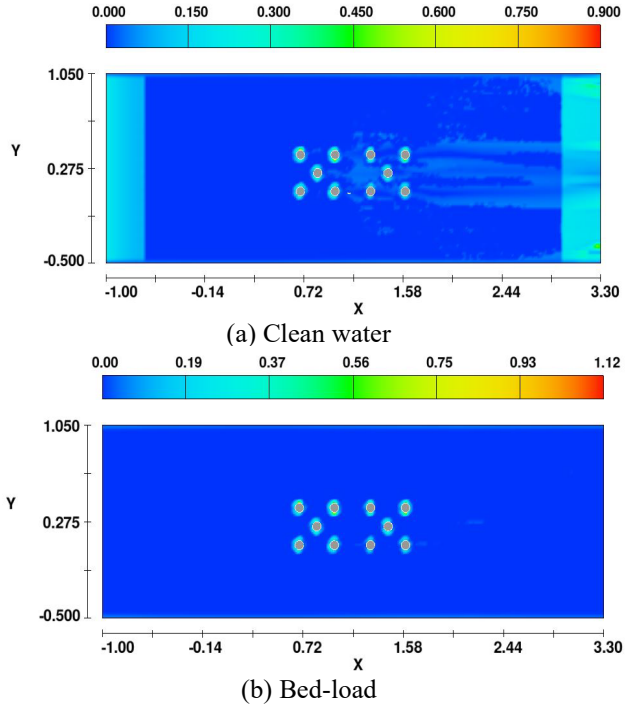

Figure 17. Distribution of shear velocity around the supports (Top section)

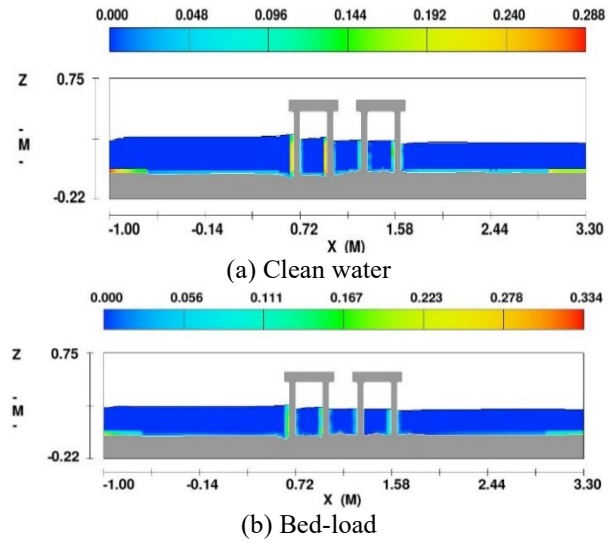

Figure 18. Distribution of shear velocity on the sides of the right side supports

Shear velocity in front of piers A1, A2, A3, B4, and B5 under both clean water and bed-load conditions was examined to assess the impact of flow on scour around the front of these supports (Figure 19). The results showed that shear velocity

under bed-load conditions was significantly higher near the piers compared to clean water conditions. It was noticed that the shear velocity at the piers A1 and A2 was approximately 19% higher when compared to pier A3. The shear velocity at the B4 and the B5 was 25% to 30% higher when compared to the front piers A1–A3. This significant increase in the shear velocity was due to the eddy effect of the turbulent flow at the piers. As the flow of water is sediment-laden, it generates more turbulence, which will increase the shear velocity at the hazards at the piers. Even this significant increase in the shear velocity was observed near the piers. It can be noticed that the scour in the rear regions was less, and that at the front regions was higher. This can be attributed to the fact that already, sediment accumulation exists in the rear regions of the piers. Because of these sediments, scour is less. Similarly, the sediment accumulation, which resulted from deposition behind the piers, was responsible for the resistance between the flow and the surface, thereby reducing the capacity of the flow to transport more sediment, thus limiting the scour in these areas. The reduction of scour in the rear areas of the piers is due to the deposition caused by the settling of sediments. In these areas, the effect of the turbulent flow diminishes because of the sediments, which accumulate to create a natural barrier to the sediment movement. The sediments accumulated increase surface friction, which does not allow the sediments to move; hence, significantly less scour occurred. These facts also justify the reasons for lower shear velocity in the rear areas of the piers under bed-load conditions, although the shear velocity increased significantly near the piers.

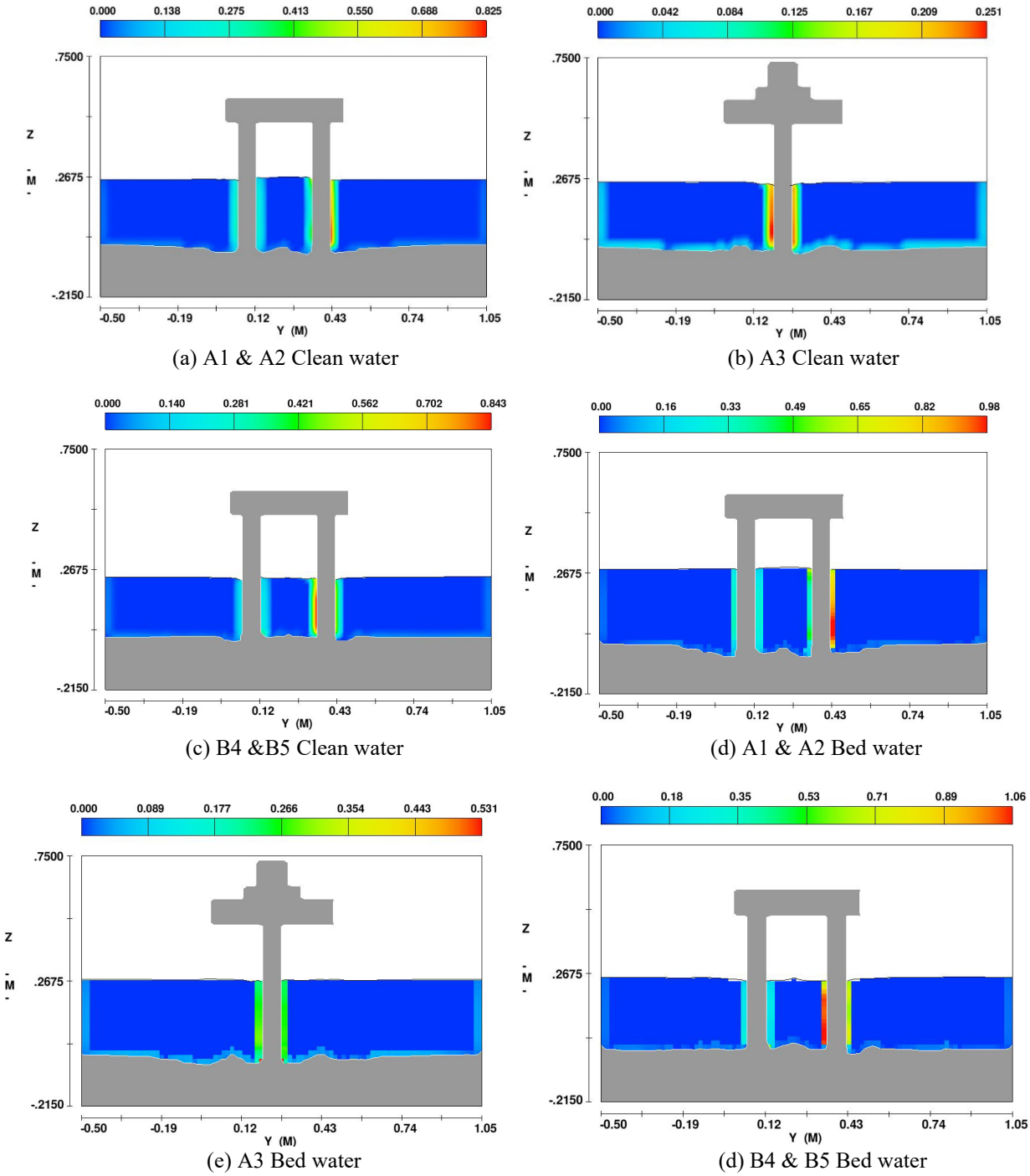

(a) A1 & A2 Clean water

(b) A3 Clean water

(c) B4 &B5 Clean water

(d) A1 & A2 Bed water

(e) A3 Bed water

(d) B4 & B5 Bed water

Figure 19. Distribution of shear on the front side

11. EVALUATION OF LIVE BED SCOUR HOLE DEPTH

Figure 20 illustrates that the flow remains directed over the water surface. With an increase in flow velocity in the regions close to the piers, the intensity of the eddies formed around the piers increases, which enhances the turbulence and shear velocity in those regions. Even though an increase in shear velocity dislodges sediments from the riverbed, the final effect of scour remains shallower than for the bed-load condition. In fact, even with high-velocity flow in clear water, the flow is not able to mobilize the sediments as in sediment-laden flow, resulting in limited scour for this case. However, under bed-load conditions in which the flow carries sediments, a massive increase in scour around the piers is found. It can be seen that shear velocity is increased notably due to the movement of the accumulated sediments that contribute to higher turbulence in the flow. In this condition, the flow can move the sediments more efficiently, forming deeper holes around the piers. Scour effects increase more for the regions with sediments due to the accumulation of sediments, which deepens the hole around the supports more than in clear water conditions due to the movement of sediments. Thus, comparing the evolution of the scour hole in both conditions:

- In clean water, the high flow velocity contributes to increased shear velocity in the areas near the piers, which removes some sediments, but the scour remains less deep compared to the bed-load condition.
- In bed-load, where the flow carries sediments, more impactful eddies are formed, enhancing scour and contributing to the formation of deeper holes around the piers. Flow velocity increases significantly due to the movement of sediments, resulting in greater scour in sediment-laden regions.

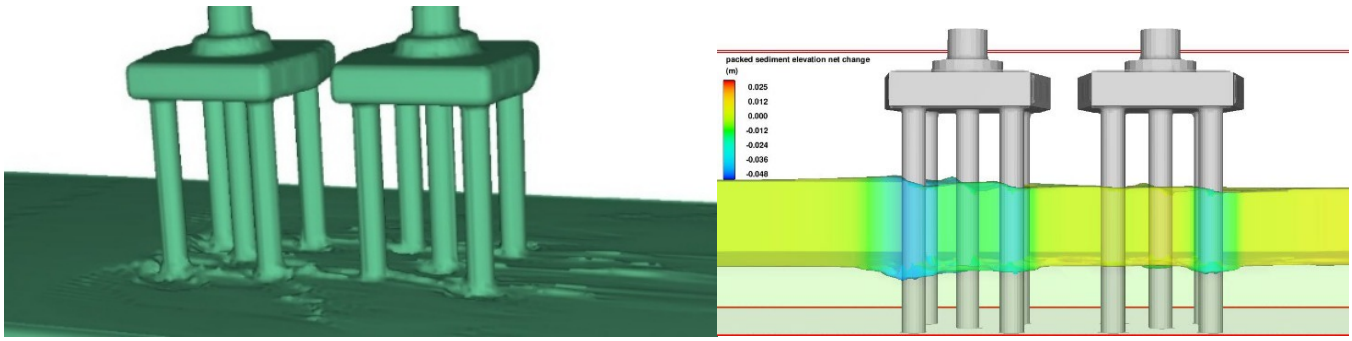

(a) Clean water

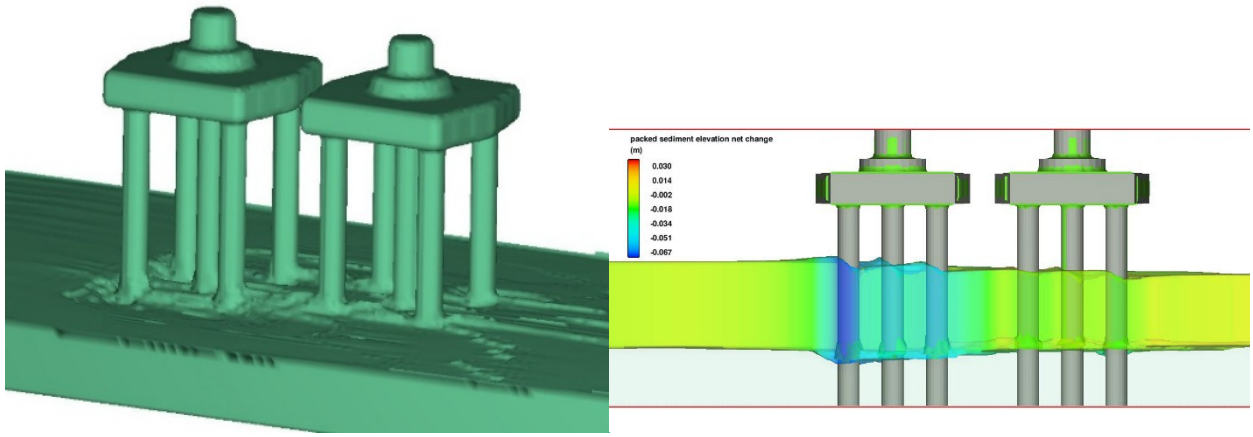

(b) Bed-load

Figure 20. The depth of the scour hole around the piers

12. CONCLUSIONS

Scour around bridge piers is an important problem in hydraulic engineering, having a direct impact on the stability of hydraulic structures. While analyzing the Tikrit Bridge in Salah al-Din Governorate, the FLOW-3D software was applied to simulate scour and compare the influence of flow on piers in a complex water environment. The study focused on the influence of sediment-laden flow (bed-load) and clean water flow on scour, considering the dynamic interaction among different piers and how they affect the movement of the flow. The simulation results underscore the importance of augmenting bridge design for turbulent flow conditions.

- The research findings showed that the improved model for calculating scour around piers using FLOW-3D provides 48% more accurate predictions of scour in areas of high-speed flow. The improvement reflects the model's ability to capture the complex interaction between piers and flow in turbulent conditions.
- The presence of more than one pier increases the complexity of flow movement and increases the scouring effect. In the case of sediment-laden flow increasing from nearly 0.12 m in the downstream group to about 0.26 m in the upstream front row (112.5% increase), more scour was observed around the piers in the high-velocity zones compared to clean water flows. All these results highlight the importance of well-spaced piers when designing bridges, thereby minimizing the influence of scouring.
- During a bed-load condition, where the flow is transporting sediment, scour was observed to increase

significantly compared to the case with clean water. It indicates that sediment-laden flow enhances the ability of the flow to transport sediment more effectively, resulting in a higher degree of scour near piers.

- Scour occurs mostly in high-velocity reaches, whereas in low-velocity sections, where the flow is not capable of transporting sediment, deposition occurs at a rate of 15–20% in sediment-laden flow. This dynamic action demonstrates the interaction between scour and deposition in complex flow conditions, such as those found in the vicinity of the Tikrit Bridge.
- Shear velocity near the piers was found to be higher under bed-load conditions (≈1.0–1.12 m/s) than in clean water (≈0.75–0.90 m/s). This stronger near-bed shear in sediment-laden flow enhances sediment entrainment, resulting in scour depths greater than those recorded under clean-water conditions.

In lateral piers, such as A1 and A4, water velocities were 15–20% higher compared to central piers, like A3 and B3, leading to increased scour in the lateral areas. Meanwhile, in central piers, velocities were 10–12% lower, resulting in a lesser scour effect in those areas.

REFERENCES

[1] Abdulkathum, S., Al-Shaikhli, H.I., Al-Abody, A.A., Hashim, T.M. (2023). Statistical analysis approaches in scour depth of bridge piers. Civil Engineering Journal, 9(1): 143-153. https://doi.org/10.28991/CEJ-2023-09-01-011

[2] Zhao, M., Zhu, X., Cheng, L., Teng, B. (2012). Experimental study of local scour around subsea caissons in steady currents. Coastal Engineering, 60: 30-40. https://doi.org/10.1016/j.coastaleng.2011.08.004

[3] Muzzammil, M., Gangadhariah, T. (2003). The mean characteristics of horseshoe vortex at a cylindrical pier. Journal of Hydraulic Research, 41(3): 285-297. https://doi.org/10.1080/00221680309499973

[4] Radice, A., Tran, C.K. (2012). Study of sediment motion in scour hole of a circular pier. Journal of Hydraulic Research, 50(1): 44-51. https://doi.org/10.1080/00221686.2011.641764

[5] Ata Amini, S., Mohammad, T.A., Aziz, A.A., Ghazali, A.H., Huat, B.B.K. (2011). A local scour prediction method for pile caps in complex piers. Proceedings of the Institution of Civil Engineers-Water Management, 164(2): 73-80. https://doi.org/10.1680/wama.900064

[6] Amini, A., Melville, B.W., Ali, T.M. (2014). Local scour at piled bridge piers including an examination of the superposition method. Canadian Journal of Civil Engineering, 41(5): 461-471. https://doi.org/10.1139/cjce-2011-0389

[7] Vijayasree, B., Eldho, T. (2016). Experimental study of scour around bridge piers of different arrangements with same aspect ratio. Scour and Erosion, 889-895. https://doi.org/10.1201/9781315375045-113

[8] Yang, Y., Qi, M., Wang, X., Li, J. (2020). Experimental study of scour around pile groups in steady flows. Ocean Engineering, 195: 106651. https://doi.org/10.1016/j.oceaneng.2019.106651

[9] Amini Baghbadorani, D., Ataie-Ashtiani, B., Beheshti, A., Hadjzaman, M., Jamali, M. (2018). Prediction of current-induced local scour around complex piers: Review, revisit, and integration. Coastal Engineering, 133: 43-58. https://doi.org/10.1016/j.coastaleng.2017.12.006

[10] Rasaei, M., Nazari, S., Eslamian, S. (2020). Experimental investigation of local scouring around the bridge piers located at a 90° convergent river bend. Sādhanā, 45(1): 87. https://doi.org/10.1007/s12046-020-1314-7

[11] Khalili, A.M., Hamidi, M., Dadamahalleh, P.A. (2024). Experimental study of the effect of rectangular debris blockage on the scour hole development around a cylindrical bridge pier. Water Practice and Technology, 19(5): 1878-1892. https://doi.org/10.2166/wpt.2024.092

[12] Hurtado-Herrera, M., Uh Zapata, M., Hammouti, A., Pham Van Bang, D., Zhang, W., Nguyen, K.D. (2024). Numerical investigation of the scour around a diamond- and square-shaped pile in a narrow channel. Ocean Engineering, 309: 118374. https://doi.org/10.1016/j.oceaneng.2024.118374

[13] Esmaeili Varaki, M., Radice, A., Samira Hossini, S., Fazl Ola, R. (2019). Local scour at a complex pier with inclined columns footed on capped piles: Effect of the pile arrangement and of the cap thickness and elevation. Journal of Hydraulic Engineering, 28(1): 91-100. https://doi.org/10.1080/09715010.2019.1702109

[14] Sheppard, D.M., Melville, B., Yang, Y. (2023). Local equilibrium sediment scour prediction at bridge piers with complex geometries. Journal of Hydraulic Engineering, 149(4): 04023003. https://doi.org/10.1061/(ASCE)HY.1943-7900.0002026

[15] Mastbergen, D.R., Van Den Berg, J.H. (2003). Breaching in fine sands and the generation of sustained turbidity currents in submarine canyons. Sedimentology, 50(4): 625-637. https://doi.org/10.1046/j.1365-3091.2003.00554.x

[16] Soulsby, R. (1997) Dynamics of marine sands: A manual for practical applications. Oceanographic Literature Review, 9(44): 947.

[17] Whitehouse, R.J.S., Soulsby, R.L., Roberts, W., Mitchener, H.J. (2000). Dynamics of estuarine muds. Technical Report, Thomas Telford.

[18] Antunes Do Carmo, J.S., Temperville, A., Seabra-Santos, F.J. (2003). Bottom friction and time-dependent shear stress for wave-current interaction. Journal of Hydraulic Research, 41(1): 27-37. https://doi.org/10.1080/00221680309499926

[19] Yass, M.F., Al-Tikrite, A. (2025). Sediment characteristics of the riverbed: The Tigris River case (Iraq). Mathematical Modelling of Engineering Problems, 12(6): 2077-2084. https://doi.org/10.18280/mmep.120623

[20] Flayyih, S.S., Jasim, F.H., Nafe'e, O.T., Jamel, A.A.J. (2025). An artificial intelligence-driven evaluation of scour depth around Bridge Piers. Engineering, Technology and Applied Science Research, 15(5): 26310-26316. https://doi.org/10.48084/etasr.12240

[21] Jamel, A.A.J., Tawfeeq, S.S., Hussain, R.A. (2025). Improving energy dissipation on stepped spillways (Numerical simulation). International Review of Civil Engineering, 16(3): 201. https://doi.org/10.15866/irece.v16i3.25616

[22] Arneson, L.A., Zevenbergen, L.W., Lagasse, P.F., Clopper, P.E. (2012). Evaluating scour at bridges (No. FHWA-HIF-12-003). National Highway Institute (US).

[23] Guo, J., Suaznabar, O., Shan, H., Shen, J. (2012). Pier Scour in Clear-Water Conditions with Non-Uniform Bed Materials.
[24] Khwairakpam, P., Ray, S.S., Das, S., Das, R., Mazumdar, A. (2012). Scour hole characteristics around a vertical pier under clear water scour conditions. ARPN Journal of Engineering and Applied Sciences, 7(6): 649-654.
[25] Sheppard, D.M., Odeh, M., Glasser, T. (2004). Large scale clear-water local pier scour experiments. Journal of Hydraulic Engineering, 130(10): 957-963. https://doi.org/10.1061/(ASCE)0733-9429(2004)130:10(957)
[26] Khassaf, S.I., Ahmed, S.I. (2021). Development an empirical formula to calculate the scour depth at different shapes of non-uniform piers. Journal of Physics: Conference Series, 1973(1): 012179. https://doi.org/10.1088/1742-6596/1973/1/012179

NOMENCLATURE

μ_f	is the drift coefficient (empirical coefficient)
θ_i, θ_{cr}, i	are the local and modified critical shear stress coefficients, respectively
v_f	it is the kinematic viscosity of the fluid
d	is the dimensionless particle size coefficient calculated from Eq. (3)
μ_f	it is the dynamic viscosity of the fluid
θ_r, θ_{cr}	the Shields coefficient and the critical Shields coefficient
τ	is the shear stress at the bottom of the turbulent flow in shallow water
g	is the magnitude of the gravity vector
d_i	is the mean particle diameter
ρ_s, i, ρ_f	the densities of the sediment and fluid